Thermal balance of a wall with PCM-enhanced thermal insulation

E. Kossecka
Institute of Fundamental Technological Research of the Polish Academy of Sciences, Warsaw, Poland
J. Kośny
Oak Ridge National Laboratory; Buildings and Materials Group, Oak Ridge, Tennessee, USA

ABSTRACT: PCM–insulation mixtures function as lightweight thermal mass components. It is expected that these types of dynamic insulation systems will contribute to the objective of reducing energy use in buildings. In this paper, dynamic thermal properties of a material in which phase change occurs are analyzed, using the temperature-dependent specific heat model. Integral formula for the total heat flow in finite time interval, across the surface of a slab of the phase change material was derived. Simulations have been performed to analyze heat transfer through a light-weight wall assembly with PCM-enhanced insulation, in different external climate thermal conditions. Results of simulations indicate that for cyclic processes, the effect of PCM in an insulation layer results in time shifting of the heat flux maxima and not in reduction of the total heat flow. The heat gains maxima, resulting in high cooling loads, are shifted in time by about two hours and reduced up to 22% for not very high external sol-air temperatures.

1 INTRODUCTION

Residential and commercial roofs and walls are currently designed and tested using steady-state criteria, with R-values based on the apparent thermal conductivity used by building standards as an important measure of energy performance. Building envelope components, however, are subject to dynamic environmental conditions. In 2002 an ORNL research team started working on fiber insulations blended with microencapsulated PCMs (Phase Change Materials) [Kosny et al. 2007a, b, 2009a, b]. These PCM–insulation mixtures function as lightweight thermal mass components. It is expected that these types of dynamic insulation systems will contribute to the objective of reducing energy use in buildings. This is a consequence of this technology's ability to reduce energy consumption for space conditioning and reshape peak-hour loads. Other anticipated advantages of PCMs include improvements towards occupant comfort, compatibility with traditional wood and steel framing technologies, and potential for application in retrofit projects. New PCM applications require careful selection of materials, identification of PCM location, bounding thermal resistances, and specification of the amount of PCM to be used.

In this paper, dynamic thermal properties of a material in which phase change occurs are analyzed, using the temperature-dependent specific heat model. Theoretical considerations are illustrated with results of simulations, performed for a light-weight wall assembly with PCM-enhanced insulation, under different external thermal excitations.

2 MODEL OF HEAT TRANSFER IN THE PCM-ENHANCED INSULATION

The heat storage capacity for a specific PCM-enhanced product is a key indicator of its future dynamic thermal performance. A theoretical model of the material with temperature-dependent specific heat can be used to calculate phase change processes in most common materials [Heim & Clarke 2004, Kissock & Limas 2006].

The one-dimensional heat transport equation for such a case is:

$$\frac{\partial}{\partial t}(\rho h)=\frac{\partial}{\partial x}\left[\lambda\frac{\partial T}{\partial x}\right] \tag{1}$$

where ρ and λ are the material density and thermal conductivity, T and h are temperature and enthalpy per unit mass. Heat flux q is given by:

$$q(x,t)=-\lambda\frac{\partial T(x,t)}{\partial x} \tag{2}$$

The enthalpy derivative over the temperature (with consideration of constant pressure) represents the effective heat capacity, with phase change energy being one of the components:

$$c_{eff}(T) = \frac{\partial h}{\partial T}. \quad (3)$$

For most PCM materials, variations of enthalpy with temperature depend to some extent on the direction of the process considered, and are different for melting and solidification. Therefore a model of the temperature-dependent specific heat, represented by an unique function of temperature, is an approximation of a real material thermal capacitance.

Figures 1 and 2 depict temperature-dependent enthalpy differences and enthalpy curves for microencapsulated PCM, generated during differential scanning calorimeter testing. In this material, the melting takes place around 27°C and solidification around 26oC. Total phase change enthalpy, H_m, within temperature interval [20o, 29o] is 122 kJ/kg.

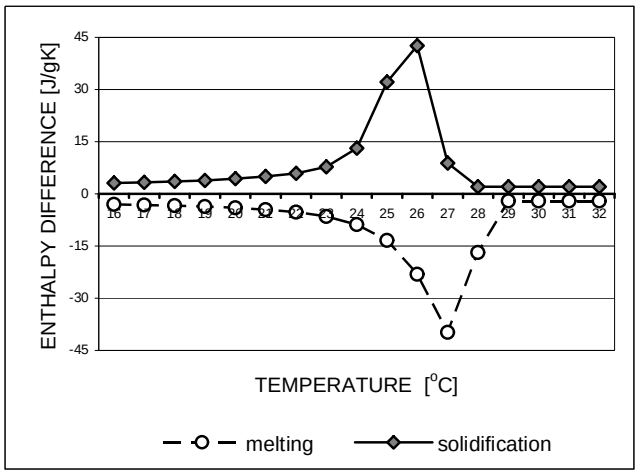

Figure 1 Calorimetric data for the microencapsulated PCM

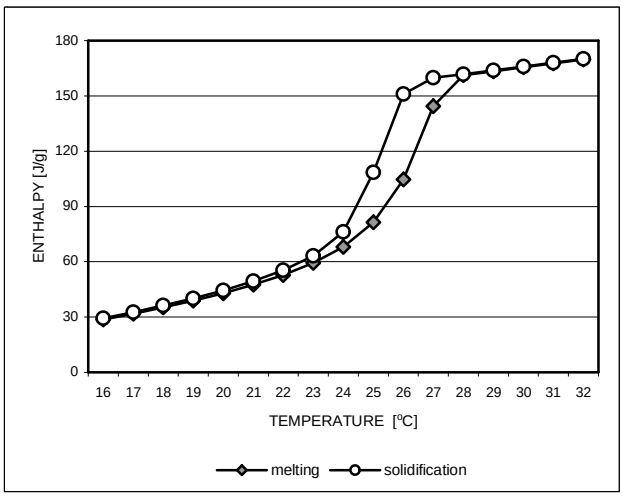

Figure 2 Enthalpy curves for the microencapsulated PCM

Effective heat capacity, c_{eff}, for a material which is a blend of insulation and PCM may be expressed as

$$c_{eff} = (1-\alpha)c_{ins} + \alpha c_{effPCM}, \quad (4)$$

where α denotes the percentage of PCM, c_{ins} the specific heat of insulation without PCM and c_{effPCM} is effective heat capacity of PCM.

In the liquid state, the effective heat capacity of PCM doesn't show temperature dependence; it may be thus represented as the sum of two terms:

$$c_{effPCM}(T) = c_l + \left(c_{effPCM}(T) - c_l\right), \quad (5)$$

where c_l represents the temperature independent specific heat in the liquid state.

For a material to be used as thermal insulation, thermal conductivity is the most important parameter, which determines its thermal performance in different thermal conditions. For cellulose fiber insulation, linear dependence of conductivity on temperature is to be observed (Kośny et al. 2009a, b):

$$\lambda(T) = \lambda_0 + \beta \cdot T \quad (6)$$

$$\lambda_0 = 0.03575; \qquad \beta = 0.00013$$

Addition of microencapsulated PCM does not result in a significant change in conductivity of the insulation.

3 THERMAL BALANCE OF A WALL WITH THE PCM-ENHANCED MATERIAL

Consider a plane wall of thickness L, composed of layers of different materials, and assume that some of them are phase change materials. Boundary (linear) conditions at the internal ($x = 0$), and external ($x = L$) surface of the wall have the form:

$$q(0,t) = \frac{1}{R_{si}}\left[T_i(t) - T(0,t)\right] \quad (7)$$

$$q(L,t) = \frac{1}{R_{se}}\left[T(L,t) - T_e(t)\right] \quad (8)$$

where T_i and T_e are ambient temperatures and R_{si}, R_{se}, surface film resistances.

Denote by $R_{i\text{-}x}$ and $R_{x\text{-}e}$ the resistances for heat transmission from the point x in the wall to the internal and external environment, respectively, and by R_u the total resistance for heat transmission through the wall. With conductivity along the wall's thickness is represented by the function of $\lambda(x)$, the resistances are given by:

$$R_{i-x} = R_{si} + \int_0^x \frac{dx}{\lambda(x)} \quad (9)$$

$$R_{x-e} = \int_x^L \frac{dx}{\lambda(x)} + R_{se} \quad (10)$$

$$R_u = R_{si} + \int_0^L \frac{dx}{\lambda(x)} + R_{se} \quad (11)$$

On multiplying Eq. (1) by the function $R_{x\text{-}e}$ and integrating with respect to x over thickness of the wall we obtain the following formula:

$$\int_0^L \rho \cdot \frac{\partial h}{\partial t} \cdot R_{x-e}\, dx = \int_0^L \frac{\partial}{\partial x}\left(\lambda \frac{\partial T}{\partial x}\right) \cdot R_{x-e}\, dx =$$

$$= \left(\lambda \frac{\partial T}{\partial x}\right) \cdot R_{x-e}\Big|_{x=0}^{x=L} + \int_0^L \frac{\partial T}{\partial x} dx =$$

$$= -R_{se} \cdot q(L) + R_{0-e} \cdot q(0) + \left[T(L) - T(0)\right] \quad (12)$$

Temperatures T(0) and T(L) may be eliminated using Eqs (7) and (8), which gives the following formula for the heat flux at internal surface:

$$q(0) = \frac{1}{R_u}(T_i - T_e) + \int_0^L \rho \frac{\partial h}{\partial t} \cdot \frac{R_{x-e}}{R_u} dx \quad (13)$$

Analogous formula for $q(L)$ is to be obtained on multiplying Equation (1) by $R_{i\text{-}x}$ and integrating by parts.

The effect of time variations of enthalpy h along thickness of the wall, on the heat flux across the surface $x = 0$, depends thus on the factor $R_{x\text{-}e}/R_u$, which takes comparatively high values, close to 1, in the vicinity of that surface and low values, close to 0, in the vicinity of the opposite surface $x = L$. This means that only time variations of enthalpy near the surface considered play an important role, whereas the effect of variations near the opposite surface may be small.

Assume now that densities and conductivities are temperature independent and thus constant in time. The last assumption should be understood as an approximation; especially in the case of insulation materials (see Eq (6)).

On performing now integration of Eq. (13) with respect to time, over the time interval $[t_1, t_2]$, and interchanging the integration order, one obtains:

$$Q(0, t_1, t_2) = \int_{t_1}^{t_2} q(0,t)\, dt \quad (14)$$

$$Q(0, t_1, t_2) = \frac{1}{R}\int_{t_1}^{t_2} \left[T_i - T_e\right] dt + \int_0^L \int_{t_1}^{t_2} \rho \frac{\partial h}{\partial t} \cdot \frac{R_{x-e}}{R_u} dt\, dx \quad (15)$$

Time integral in the second term represents the enthalpy difference Δh; it can be expressed as follows:

$$\Delta h(x, t_1, t_2) = \int_{t_1}^{t_2} \frac{\partial h}{\partial t} dt = \int_{t_1}^{t_2} \frac{\partial h}{\partial T} \frac{\partial T}{\partial t} dt = \int_{T(x,t_1)}^{T(x,t_2)} c_{eff}(x,T)\, dT \quad (16)$$

Integration of $c_{eff}(x,T)$ over temperature can be conducted when the final temperature distribution in the slab is known. For particular heat transfer processes, it is possible to determine the enthalpy difference Δh without performing detailed simulations. Taking into account Eq. (15), the total heat flow in time interval $[t_1, t_2]$ across the surface $x = 0$ is given by:

$$Q(0, t_1, t_2) = \frac{1}{R_u} \int_{t_1}^{t_2} \Delta T_{i-e}(t)\, dt + \Delta H_{s0} \quad (17)$$

$$\Delta T_{i-e}(t) = T_i(t) - T_e(t) \quad (18)$$

$$\Delta H_{s0}(t_1, t_2) = \int_0^L \rho\, \Delta h(x, t_1, t_2) \cdot \frac{R_{x-e}}{R_u} dx \quad (19)$$

ΔH_{s0} represents that part of the total enthalpy difference in a slab which is due to the heat flow across the surface $x = 0$. For cyclic processes, if time integration is over integral number of cycles, $\Delta H_{s0} = 0$, and total heat flow depends on the mean ambient temperature difference.

4 TIME CONSTANT OF A PCM SLAB

Assume that the heat flux course, $q(t)$, across the unit surface area of the slab at the cold side, after a step function temperature excitation at the opposite, hot side, as a function of time t may be approximately described as a simple relaxation process, with the time constant τ_s:

$$q(t) \approx \frac{\Delta T}{R}\left[1 - \exp\left(-\frac{t}{\tau_s}\right)\right] \quad (20)$$

The total heat flow in time interval $[0, t]$ is given by:

$$Q(t) \approx \frac{\Delta T}{R}\left[t - \tau_s\left(1 - \exp\left(-\frac{t}{\tau_s}\right)\right)\right] \quad (21)$$

For time t sufficiently long, as compared with τ_s, the steady state of heat flow is attained, and $Q(t)$ may be approximated by:

$$Q(t) \approx \frac{\Delta T}{R}(t - \tau_s) \quad (22)$$

Comparison of (17) and (22) yields:

$$\tau_s = R \cdot \frac{\Delta H_{s0}}{\Delta T} \quad (23)$$

In earlier work of Kossecka and Kosny (2008) a similar analysis was used for estimating the time constants for conventional non-PCM assemblies, for purposes of the hot-box test measurements. However, in the case of a PCM specimen, the time constant is strongly dependent on its enthalpy difference within the temperature interval taken into account.

Figure 3 depicts comparison of heat fluxes across surfaces of insulation layer of thickness 0.14 m, with no PCM and 30% content of PCM, after the temperature rapid jump, from initial temperature of 14°C to final temperature of 44°C. (Insulation thermophysical properties as in Table 1, PCM enthalpy data as represented in Figure 1). The time constant, τ_s, estimated using Eqs. (16), (19) and (23), was about 56 min for pure insulation and 153 min for insulation with 30% PCM.

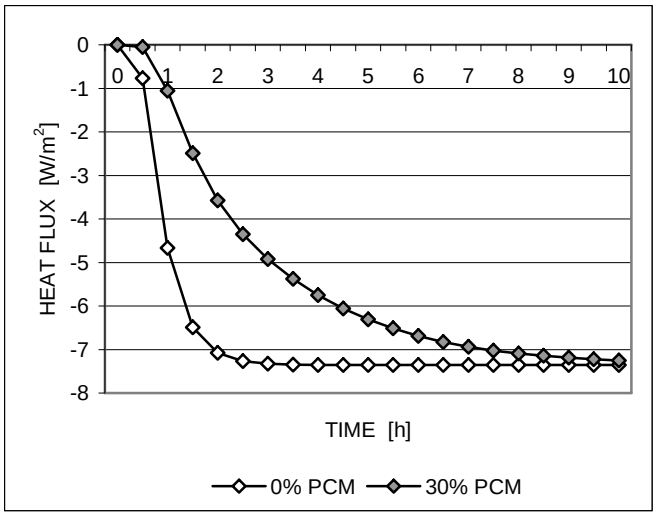

Figure 3 Heat fluxes across the surface of an insulation layer after temperature jump at the opposite surface

5 PERFORMANCE OF THE PCM-ENHANCED INSULATION IN DIFFERENT CLIMATE CONDITIONS

Simulations have been carried out to demonstrate the performance of a light-weight wall assembly with PCM-enhanced insulation in different external climate thermal conditions. The "melting curve" of Figure 1 has been assumed as a model of the PCM effective heat capacity. Temperature dependence of thermal conductivity was represented by Eq (6).

Wall assembly similar to a typical 14 cm (5.5 in) wood frame wall has been considered. Thermophysical properties of the wall's layers are listed in Table 1. Total resistance for heat transfer, including surface film resistances R_{si} = 0.13 m^2·K/W and R_{se} = 0.04 m^2·K/W, R_u = 4.14 m^2·K/W, and U-value is 0.24 [W/m^2·K]. PCM content of 30% in an insulation layer of thickness of 0.14 m and density of 33.6 kg/m^3 means about 1.4 kg of PCM per square meter of a wall.

Table 1 Thermophysical properties of the wall's layers

Material	L m	λ W/(m·K)	ρ kg/m^3	c_p kJ/(kg·K)
Gypsum board	0.013	0.16	800	1.088
Insulation	0.140	0.039	25.6	1.381
Ins. 30% PCM	0.140	0.039	33.6	$c_p(T)$
Plywood	0.013	0.12	544	1.244
Wood siding	0.013	0.07	545	1.255

One-dimensional heat transfer has been assumed and the effect of studs has been neglected. The idea was to analyse dynamic responses of a wall due to the external thermal excitation, T_e, representing the diurnal temperature swing and thermal peak, as one due to solar radiation incident on the external surface, during the day-time. Internal temperature, T_i, has been set constant at the same time.

In the linear model, when the heat flux due to solar radiation absorbed at the wall's surface, q_s, is included, boundary condition (7) takes the form:

$$q(L) = \frac{1}{R_{se}}\left[T(L) - T_e\right] - q_s = \frac{1}{R_{se}}\left[T(L) - T_{es}\right] \quad (24)$$

$$T_{es} = T_e + R_{se} \cdot q_s \quad (25)$$

T_{es} is the so called sol-air temperature. With R_{se} = 0.04 m^2·K/W, solar radiation flux of 1000 W/m^2 increases T_{es} by 40ºC.

The external (sol-air) temperature profiles, assumed in simulations, were thus as follows.

During night-time: $t < 6$ h or $t > 18$ h

$$T_{es} = T_{e0} - A_1 \cdot \sin\left[\pi \cdot (t+6)/12\right]$$

During day-time: 6ºh ≤ t ≤ 18ºh

$$T_{es} = T_{e0} - (A_1 + A_2) \cdot \sin\left[\pi \cdot (t+6)/12\right]$$

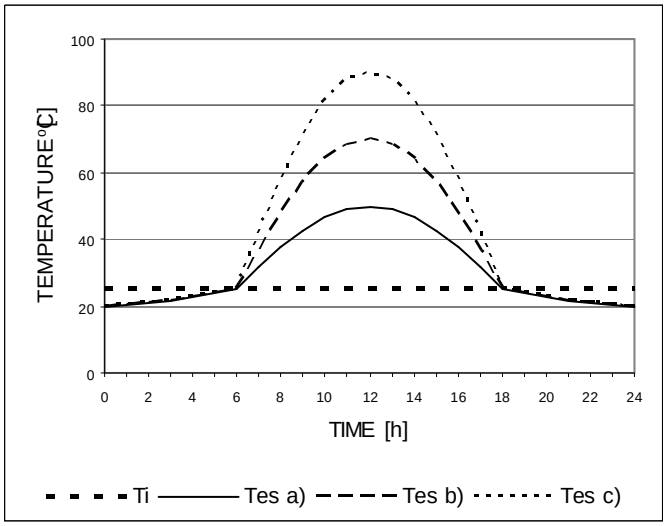

Figure 4 Internal and external temperature daily profiles (T_i = 25ºC)

Two series of simulations have been performed for T_i = 20ºC, T_{e0} = 20ºC and T_i = 25ºC, T_{e0} = 20ºC, with amplitudes values A_1 = 5ºC and A_2 = 20ºC, 40ºC and 60ºC, subsequently. Simulation cycles have been repeated, to minimize the effect of initial conditions.

To visualize dynamic effects, heat fluxes for steady state, which represent the "zero mass" wall, were calculated, taking into account dependence of insulation conductivity on temperature. An accurate elementary solution of the non-linear steady state heat transfer problem, in the case of linear dependence of conductivity on temperature, may be obtained using the Kirchoff transform method; see Kossecka (1999).

Figures 5-6 a,b,c represent comparison of diurnal heat flux profiles at internal surfaces of two walls; one containing plain fiber insulation layer, and another one containing 30% PCM enhanced insulation. The steady state heat flux profiles were added for comparison.

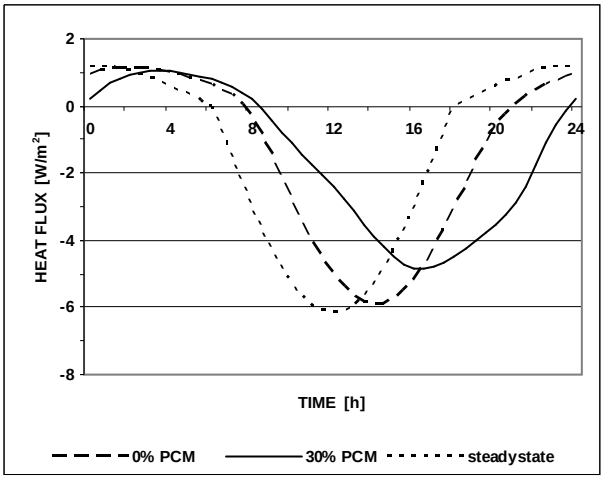

a)

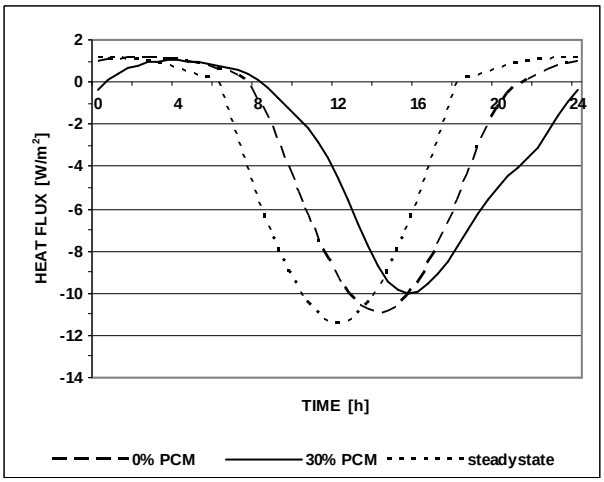

b)

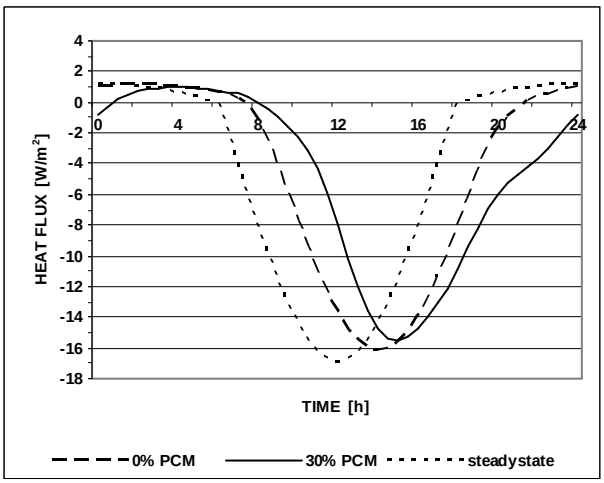

c)

Figure 5 a, b, c Comparison of the daily heat flux profiles at the internal surface of the wall containing 0.14 m thick insulation layer with 0% PCM and 30% PCM for T_i = 20ºC and A_2 = 20ºC(a), 40ºC(b) and 60ºC(c)

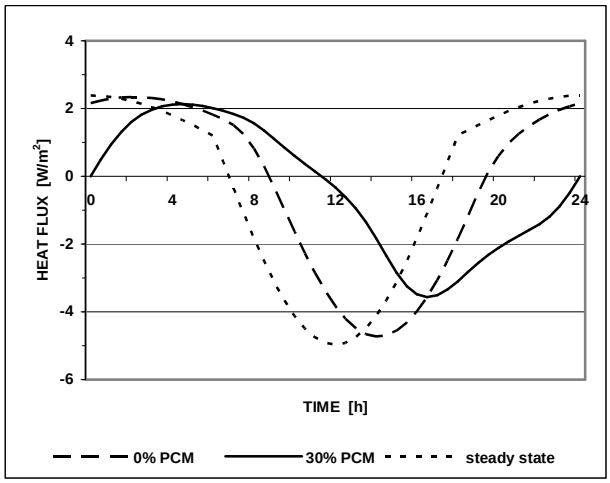

a)

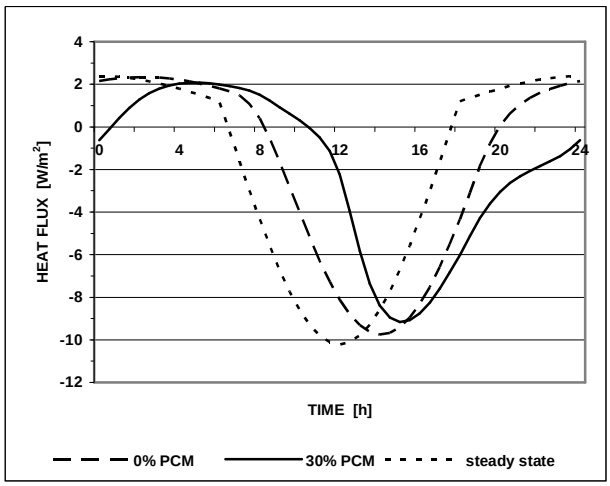

b)

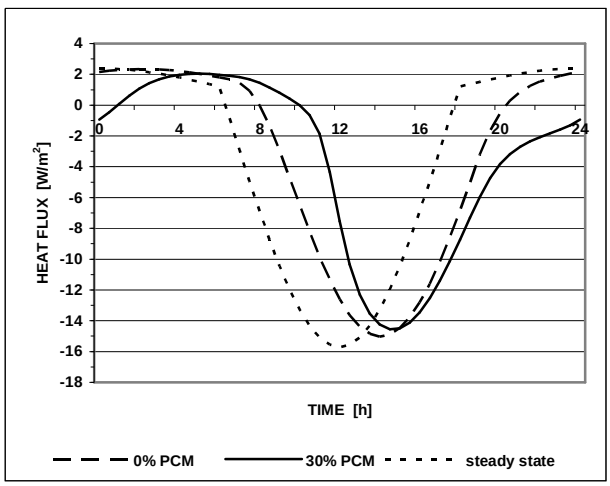

c)

Figure 6 a, b, c Comparison of the daily heat flux profiles at the internal surface of the wall containing 0.14 m thick insulation layer with 0% PCM and 30% PCM for T_i = 25ºC and A_2 = 20ºC(a), 40ºC(b) and 60ºC(c)

Comparison of the plots and calculated daily heat flow values indicates that for cyclic processes the effect of PCM in an insulation layer results in time shifting of the heat flux maxima and not in reduction of the total heat flow. Heat losses corresponding to minimum external temperatures at midnight are shifted to morning time, at the same time large heat

gains from midday are shifted by about two hours to the afternoon time.

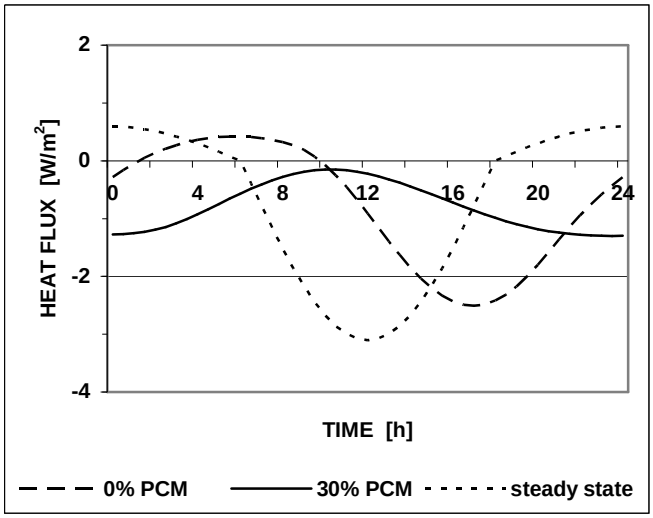

a)

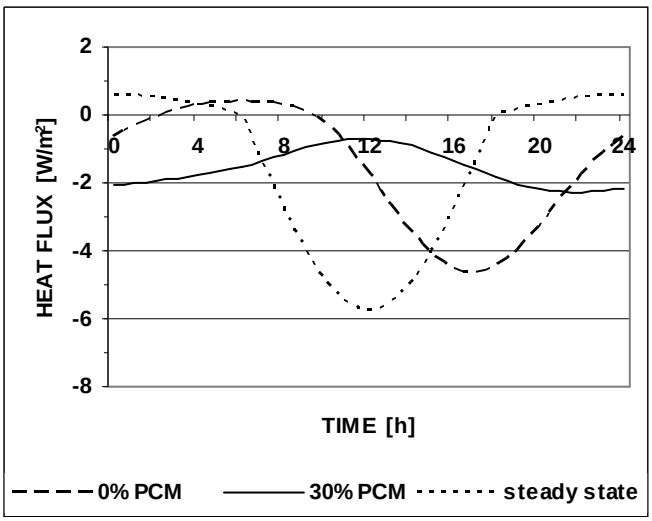

b)

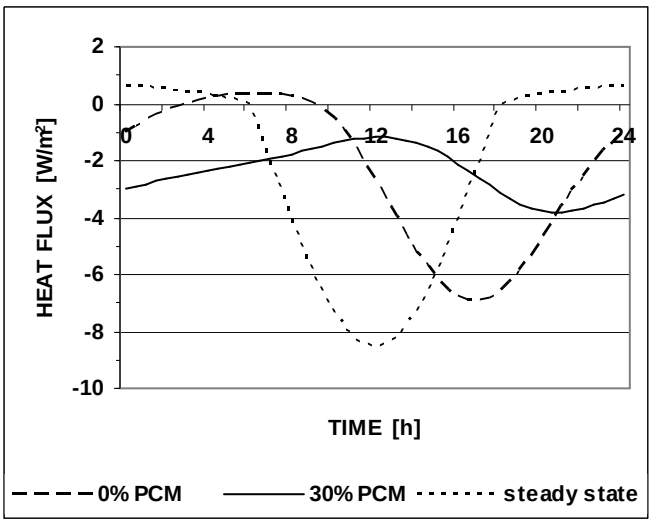

c)

Figure 7 a, b, c Comparison of the daily heat flux profiles at the internal surface of the wall containing 0.3 m thick insulation layer with 0% PCM and 30% PCM for T_i = 20oC and A_2 = 20oC(a), 40oC(b) and 60oC(c)

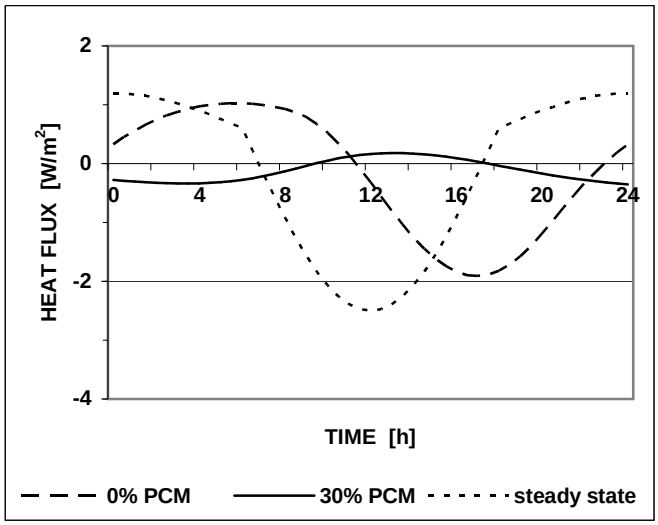

a)

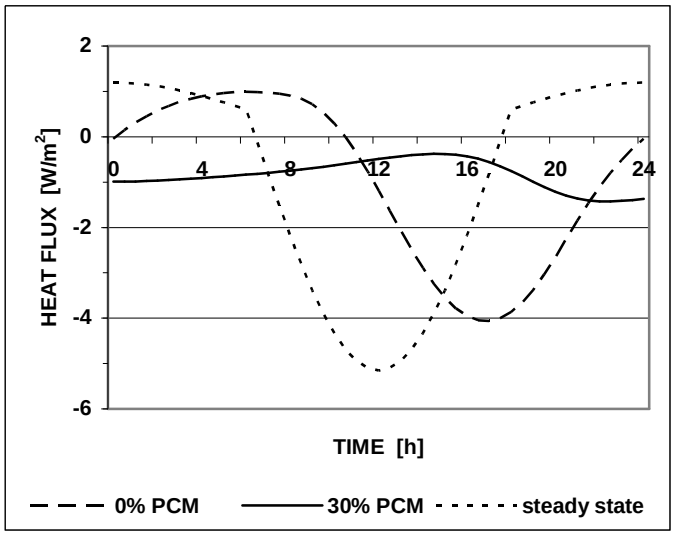

b)

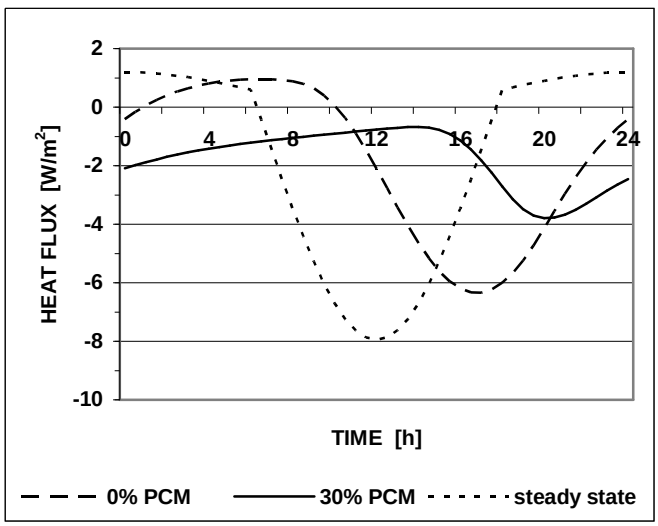

c)

Figure 8 a, b, c Comparison of the daily heat flux profiles at the internal surface of the wall containing 0.3 m thick insulation layer with 0% PCM and 30% PCM for T_i = 25oC and A_2 = 20oC(a), 40oC(b) and 60oC(c)

For T_i = 20oC the heat gains maxima are reduced by 18%, 8% and 4%, as external sol-air temperature maxima increase from 45oC to 85oC, and for

T_i = 25oC by 25%, 6% and 3% as those maxima increase from 50oC to 90oC. The effect of PCM in an insulation layer is thus positive, but perhaps not as strong as one would expect. An amount of the PCM in the insulation layer of about 1.4 kg/m^2 can not reduce much high negative heat fluxes, resulting in cooling loads on the room space, for very high external sol-air temperatures.

Simulations have been repeated for the wall containing the insulation layer of thickness 0.3 m. With PCM content of 30% and density of 33.6 kg/m^3 this means about 3 kg of PCM per square meter of a wall.

Figures 7-8 a,b,c represent, as before, comparison of diurnal heat flux profiles at internal surface of the wall, for different internal and external sol-air temperature courses. Reduction of the heat gains maxima is now 48%, 51%, 45% for T_i = 20oC, and 82%, 65%, 40% for T_i = 25oC.

CONCLUSIONS

Results of simulations are consistent with results of theoretical considerations presented in section 2. Comparison of the plots and calculated daily heat flow values indicates that for cyclic processes the effect of PCM in an insulation layer results in time shifting of the heat flux maxima and not in reduction of the total heat flow.

For insulation thickness of 0.14 m reduction of the heat gains maxima, compared to plain cellulose fiber insulation, is significant only when the external sol-air temperature amplitude if not too high (up to 25oC); for very high external temperature peaks its rather small.

The situation is much better for very thick PCM enhanced insulation layer. In this case, reduction of the heat gains maxima, compared to plain cellulose fiber insulation, is about 50% or more.

REFERENCES

Evers A.C., Medina M.A., Fang Y. 2010. Evaluation of the thermal performance of frame walls enhanced with paraffin and hydrated salt phase change materials using a dynamic wall simulator, *Building and Environment* 45, 1762-1768.

Heim, D. & Clarke, J.A. 2004. Numerical modelling and thermal simulation of PCM-gypsum composites with ESP-r, *Energy and Building*, 36, 795-805.

Kissock K., Limas S. 2006. Diurnal load reduction through phase-change building components. *ASHRAE Transactions* 112(1), 509–517.

Kosny J., Yarbrough D, Petrie T.W., Syad A. 2007a. Performance of Thermal Insulation Containing Microencapsulated Phase Change Material, presented at 2007 International Thermal Conductivity Conference.

Kosny J., Yarbrough D., Miller W., Petrie T., Childs P., Syad A. 2007b. Thermal Performance of PCM-Enhanced Building Envelope Systems, X Thermal Envelopes Conference.

Kośny J., Yarbrough D.W., Miller W.A., Wilkes K.E., Lee E.S. 2009a. Analysis of the dynamic thermal performance of fiberous insulations containing phase change materials, 11th International Conference on Thermal Energy Storage; Effstock 2009 - Thermal Energy Storage for Energy Efficiency and Sustainability, Stockholm, Sweden.

Kośny J., Yarbrough D.W., Kossecka E. 2009b. Use of a Heat-Flow Meter to Determine Active PCM Content in an Insulation. 30th International Thermal Conductivity Conference, Pittsburgh, PA USA.

Kossecka E. 1998. Relationships between structure factors, response factors and z-transfer function coefficients for multilayer walls. ASHRAE Transactions 104(1), ,68-77.

Kossecka E. 1999. Method of Averages to Determine Insulation Conductivity under Transient Conditions, *Journal of Thermal Insulation and Building Science*, Vol. 23, s. 145-158.

Kossecka E. & Kośny J. 2002. Influence of insulation configuration on heating and cooling loads in a continuously used building, *Energy & Buildings*; Vol. 34, No. 4, 321-331.

Kossecka E. & Kośny J. 2008. Hot Box Testing of Building Envelope Assemblies; a Simplified Procedure for Estimation of Minimum Time of the Test; *Journal of Testing and Evaluation*, Vol. 36, Issue 3, 242-249.

Kossecka E. & Kośny J. 2009. Dynamic test method of PCM content in fiberous insulation [in Polish], *XII Conference Building Physics in Theory and Practice*, Lodz University, Poland.

Zhu N., Ma Z., Wang S. 2009. Dynamic characteristics and energy performance of buildings using phase change materials: A review. *Energy Conversion and Management* 50, 3169–3181.